Nima Zoghipour
Akif Furkan Yaratan
Ferhat Çelik

Torun Bakır Alaşımları
Metal San. Ve Tic. A.Ş.
Kocaeli

Yusuf Kaynak

Marmara Üniversitesi
Makine Mühendisliği Bölümü
İstanbul

Makale Bilgisi:
Araştırma Makalesi
Gönderilme: 23-02-2021
Kabul: 11-03-2022

*Sorumlu Yazar: Nima ZOGHİPOUR
Email: nima.zoghipour@gmail.com

Influences of Cutting Strategies and Parameters on Tool Wear in Threading Operation of 316L Stainless Steel

External threading is one of the most relevant operations in machining. Despite of the development of new technologies and knowledge including tool geometries in micro scale, and new coating materials and grades, tool wear increases rapidly, and the tool life can be as short as just a few minutes in threading operation of hard-to-cut materials such as stainless steel. Moreover, tool wear influences the workpiece geometrical accuracy and surface quality of the machined specimens. Current work investigates the effects of various cutting strategies and parameters on the tool wear during external threading operation of AISI 316L stainless steel. The wear rate and mechanism have been evaluated on the nose, left and right sides of the cutting edges. The tool wear problem has been evaluated through desirability function optimization method. Furthermore, empirical models have been developed for prediction of the wear rate.

Keywords: Threading, stainless steel, cutting strategy, tool wear, optimization.

Atıf şekli/How to cite: Zoghipour, N., Yaratan, A. F., Çelik, F., Kaynak, Y., Influences of Cutting Strategies and Parameters on Tool Wear in Threading Operation of 316L Stainless Steel, Makina Tasarım ve İmalat Dergisi, 20 (2022) 2, 29-35.

INTRODUCTION

Austenitic stainless steels are well-known materials in various fields including aeronautical, biomedical and marine technology due to their high mechanical strength and corrosion resistance [1]. Several manufacturing processes are applied to those materials before delivery for the final use. Threading is divided into external and internal (tapping) categories. External threads can be manufactured by cutting or form rolling processes. External threading operation is one of the most important machining processes in order to manufacture and assemble parts with high accuracy and surface quality. Threading operation is generally executed on machining center or by turning machines in which cutting velocity and feed play the major roles in the process. The synchronism between spindle speed and feed rate is the most important relation in threading and tapping processes because when this relation is out of pattern, significant thread profile error occurs since the feed is equal to the pitch size and spindle speed completes the cutting form according to the standards of the thread [3]. Tool wear and surface quality are the main outputs which should be taken into evaluation in the threading operation. Excessive wear during the operation can lead to tool breakage due to the change in the contact area of the cutting insert and workpiece or deterioration in the thread profile and geometry. Corruption of the thread is reliant on the threading tools geometry. Sharp cutting edges will in general deliver articulated feed imprints and more serious surface deterioration (e.g., tears, laps, pits, breaks, and so on) than honed edges because of increased stresses at the confined tool-chip and tool–workpiece contact areas [2].

Siqueira et al. [3] analyzed the tapping process with two types of taps in SAE 1020 steel considering the torque and thrust force. Their results demonstrated that torque and thrust force variates with the change in cutting speed, coating, and chip breaker type. Taps with higher helix angle, without chip breaker, and coated were the best option for tapping in threaded blind holes. Junior et al. [4] studied the tool wear and the thread profile during machining of metric threads in square plate stainless steel in dry and emulsion condition using optical microscope and scanning

electron microscopy. According to their results, considering the cooling system, tool wear demonstrated a significant variance. However, the tool wear had not proved to be a determining factor in defining tool life. Ondin et al. [5] studied the turning of the PH 13-8 Mo stainless steel. Their results showed that the adhesion mechanism is highly active in stainless steel. The adhesion mechanism leads to a change in the cutting-edge geometry, reduction in the tool cutting capacity, and increase in the cutting forces and chatter. Pierra et al. [6] investigated the process behavior regarding the secondary and uncontrollable characteristics, such as thread length, tool coating, feed rate, and hole's diameter for internal thread process with cut and form taps. Furthermore, they studied the behavior of a new type of floating system in terms of torque and axial force. Akyildiz et al. [7] predicted the thread cutting forces by dividing the thread chip into three parts, one thread root and two side faces. They studied the chip compression ratios for the V-shaped single piece and separately cut chip zones are measured and cutting forces are calculated and compared for precision metric thread cutting on a SAE 4340 steel bar. Astakhov et al. [8] studied the effects of the feed, edge, inclination, and rake angles; and calculated cutting forces using empirical models.
Proper selection of tool orientation, geometry, coating type, cutting strategy, active cutting edge and cutter-workpiece engagement can lead to improvements in the machined workpiece surface quality and tool life besides to the substantial savings in machining time, and lastly leading to higher productivity rates and overall cost reduction. Consequently, most of the researchers have studied the cutting forces and thread profiles. However, there is no available research papers on the effects of the cutting strategies with different parameters until the execution of the current work.

In this work, it has been focused on the effects of different cutting strategies and parameters on the tool wear during external threading operation of AISI 316L stainless steel. EspritCam 2017 software has been taken advantage in order to study the effects of different thread cutting strategies. Furthermore, the problem has been evaluated through desirability function optimization method.

METHODOLOGY

EXPERIMENTAL PROCEDURE

In this study, the work material was X2CrNiMo17-12-2 (1.4404) AISI 316L with a diameter of 25 mm bar. The chemical composition and mechanical properties of the test material is given in Table 1. The machining tests were performed on 7 axis SR-32J/JN CNC Swiss-type Automatic Lathe. The cutting insert was PVD TiAlN coated 60˚ form type Sandvik 266RG-16MM01F100E 1135. M24×1 male thread was applied on the workpiece. The cutting speed and toolpath quantity were set to be 70 and 120 m/min, 4 and 8, respectively. Four cutting strategies; namely, off, left, right and zig-zag were utilized in order to generate G-codes. In off mode, the tool is positioned at the center of the thread. Both sides of the tool engage the material. In left mode, each cutting pass starts along the left edge of the thread. All cutting takes place on the right side of the tool. In right mode, each cutting pass starts along the right edge of the thread. All cutting takes place on the left side of the tool. In zig-zag mode, cutting passes alternate between left and right. The final pass is positioned at the center of the thread. Figure 1 demonstrates the difference in the mentioned cutting strategies [10]. The depth of cut was set to be even chip cross section. In this setting, the depths of cut are calculated to maintain a constant tool load, causing the incremental depth to become smaller as the tool goes deeper into the material [10].

Table 1 Chemical composition of the studied stainless steel [9]

AISI 316L			
Composition	Percentage	Technical Specifications	
C	0.016	Tensile Strength (MPa)	650
Mn	1.6		
P	0.038	Hardness HBW	192
S	0.030		
Si	0.36	Density (g/cm3)	8
Cr	16.7		
Ni	10.7	Machinability	Medium
Mo	2.02		

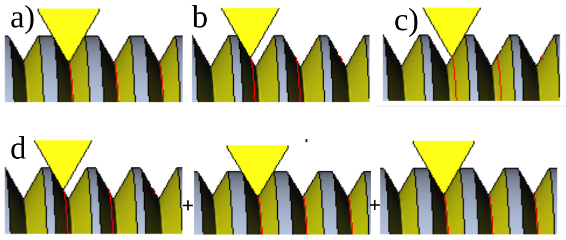

Figure 1. Different thread cutting strategies; a) off, b) left, c) right, d) zig-zag [10]

It is worthy to mention that the off mode generates G92 codes while the generated codes using other modes are at G32 format.

G92 X.. Z.. F..

G32 X.. Z.. F..

where;

X = Current diameter of the thread pass

Z = End position of the thread in Z-axis

F = Threading feed rate in in/rev (Thread Pitch)

Both coding methods are utilized in longitudinal, transverse, tapered threads, single and multiple start threads with a constant pitch, and lastly variable pitch and taper angles by chaining thread cutting blocks. G33/G32 is used for thread cutting, but with G33/G32 a single threading cut is performed. In other words, the positioning of the cutter is entered by the operator or CAM program. G76 is more used as the upgraded version of G33/G32 threading cycles [11].

RESULTS AND DISCUSSION

The nose and flank wear of two edges of the insert was inspected by using KEYENCE VHX-6000 digital optic microscope. Table 2 illustrates the measured wear results after threading operation of 60 mm. Figure 2 demonstrates the measured wear of the insert for the related experiment.

The highest nose wear has been observed as 57 µm in off mode, 120 m/min and 4 passes. However, the lowest was equal to 16 µm in left mode, 70 m/min and 8 passes. The highest flank wear on the right edge of the insert has been observed as 43 µm in off mode, 120 m/min and 4 passes consisting of 3 rough and one finishing passes. However, the lowest was equal to 14 µm in left mode, 70 m/min and 8 passes consisting of 6 rough and 2 finishing passes. The highest flank wear on the left edge of the insert has been observed as 39 µm in off mode, 120 m/min and 4 passes. However, the lowest was equal to 10 µm in left mode, 70 m/min and 8 passes. Increasing the cutting speed has concluded to a boost in the wear rate which can be attributed to the increase in temperature between tool face and the workpiece and occurring chemical reactions and diffusion. In contrary, increasing the pass quantity during threading operation has improved the tool life in terms of wear resistance which can be attributed to the reduction in the contact area between tool face and workpiece due to the depth of cut.

As it seen in Figure 2 (2), using higher cutting speed and low pass quantity has resulted in the breakage of the insert nose since in off mode, the feeding of the tool is in radial direction. Therefore, the workpiece material is cut in both sides of the thread flanks and the chip breakability using this strategy is low. The high contact area of the insert nose and flank edges leads to higher temperatures and stresses and subsequently shorter tool life.

Table 2 The measured wear after of the insert threading operation

Run	Strategy	Vc (m/min)	Pass Quantity	Nose wear (µm)	Wear flank-right (µm)	Wear flank-left (µm)
1	Off	70	8	30	24	29
2	Off	120	4	57	43	39
3	Left	70	8	16	14	10
4	Left	120	4	42	33	21
5	Right	70	4	24	28	18
6	Right	120	8	49	38	27
7	Zig-zag	70	4	25	31	32
8	Zig-zag	120	8	54	42	33

Looking to the Figure 2 (3), (4), (5) and (6), using left cutting strategy has resulted in just a little bit lower wear rates compared to the right one considering nose, right and left flank edges wears. This can be attributed to the motion direction of the tool and workpiece. In left and right modes, the feed direction is parallel to one of the thread flanks. The chip breakability and flow from the cutting edge, leading to a convenient heat transformation/dissipation. The only disadvantage of this strategy is the low surface quality of the machined surface due to the smearing of the trailing edge along the flank edge instead of cutting. Moreover, built up edge has occurred on the insert cutting edges using right mode.

Another insert nose breakage has been observed in run #8. In zig-zag mode, the feed direction of the tool is along both sides of the thread flanks. Then, both sides of the flank edges cooperate in the cutting process. The lower chip flow and breakability is the disability resulting in low surface quality and cutting tool breakage due to the applied high stress of the chip stuck on the insert. Thus, machining of large pitches and for such thread forms as acme and trapeze using this cutting strategy is appropriate [12].

As it is seen form Figure 2, chips and material adhesions are observed on the rake surface in almost all runs resulting in fractures in the cutting tools. Figure 3 shows a detailed view of a tool that was affected by nose wear and build-up edge. In experiments using low cutting speeds, the occurrence of the BUE (Build-up edge) phenomenon, which is the agglomeration of machined material on the rake face of the tool leading to seize of the tool tip, separating it from the chip, was expected at higher rates as compared to the experiments using high cutting speed. However, geometrical deterioration and deformation of the cutting tool due to the BUE phenomenon was greater at 120 m/min cutting speed than 70 m/min cutting speed. It was observed in all experiments that the BUE effect on this material could not be neglected at both cutting speeds. As shown in Figure 4, the cutting surface deteriorates after BUE formation, and then it causes fracture in the nose of the cutting tool that in cutting parameters that require high force (at Vc=120 m/min; Nap=4) and in cutting strategies which are defined as Off and Zigzag. After these fractures, it has been observed that the BUE phenomenon occurs on the cutting edge of the cutting tool, especially in runs No. 8 and 2.

DEVELOPMENT OF THE EMPIRICAL FIT MODELS FOR WEAR RATE

In this section empirical fit models have been developed for each cutting strategy as illustrated between Equation 1 and 9. The R2 of the models are 0.9974, 0.9996, and 0.9733 for nose, right and left flank edges, respectively.

Strategy: Off

$$W_{nose}=-7.7000+0.5350V_c+0.0625Nap \tag{1}$$

$$W_{right}=11.8500+0.2950V_c-1.0625Nap \tag{2}$$

$$W_{left}=23.4000+0.1550V_c-0.6875Nap \tag{3}$$

Strategy: Left

$$W_{nose}=-22.2000+0.5350V_c+0.0625Nap \tag{4}$$

$$W_{right}=1.8500+0.2950V_c-1.0625Nap \tag{5}$$

$$W_{left}=4.9000+0.1550V_c-0.6875Nap \tag{6}$$

Strategy: Right

$$W_{nose}=-14.7000+0.5350V_c+0.0625Nap \tag{7}$$

$$W_{right}=11.3500+0.2950V_c-1.0625Nap \tag{8}$$

$$W_{left}=11.9000+0.1550V_c-0.6875Nap \tag{9}$$

Strategy: Zig-zag

$$W_{nose}=-11.7000+0.5350V_c+0.0625Nap \tag{10}$$

$$W_{right}=14.8500+0.2950V_c-1.0625Nap \tag{11}$$

$$W_{left}=21.9000+0.1550V_c-0.6875Nap \tag{12}$$

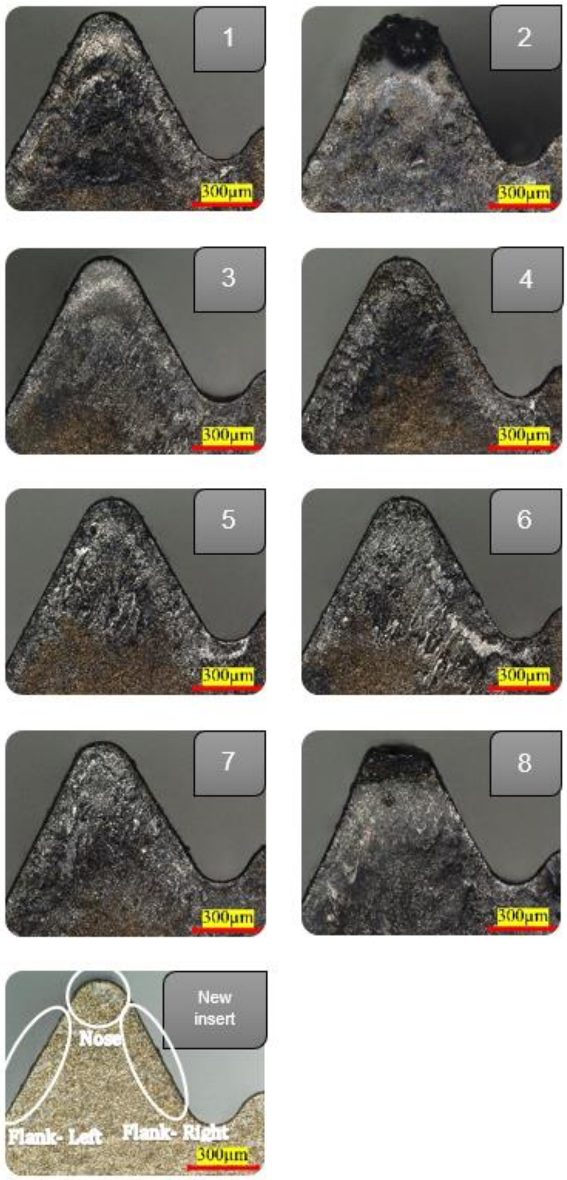

Figure 2. The wear images of the threading insert

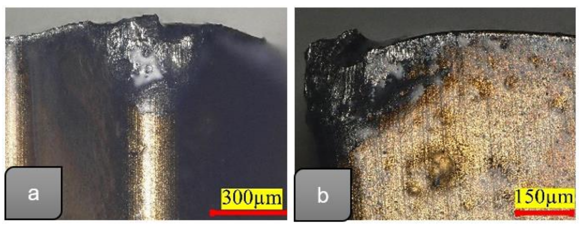

Figure 3. The wear images of the threading insert for run No. 2; a) View on tool nose, b) View on the flank

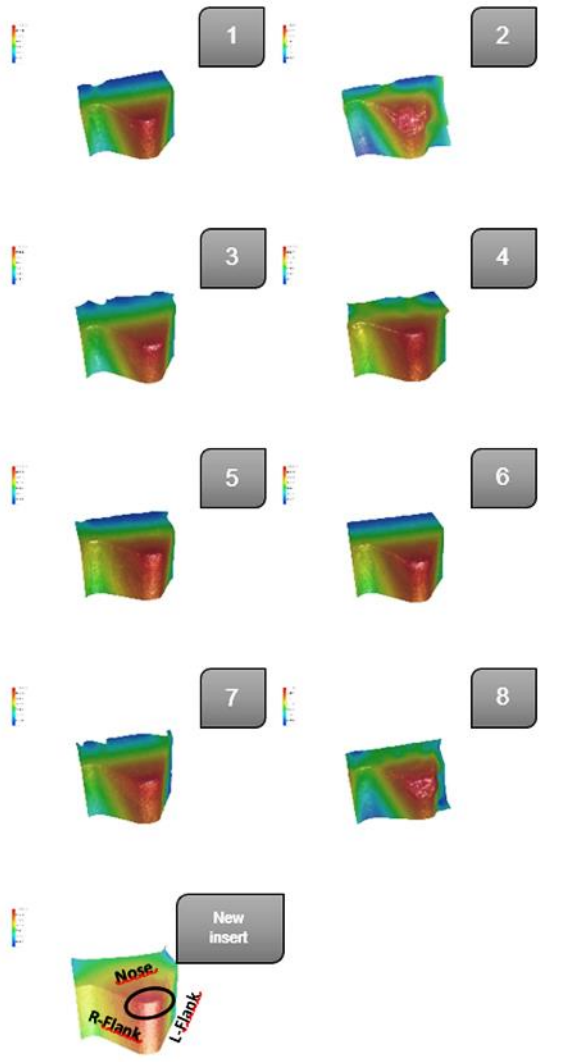

Figure 4. The wear 3D images of the threading insert

OPTIMIZATION OF THE WEAR RATE USING DESIRABILTY FUNCTION

In the desirability function approach, every reaction is changed into a desirability esteem (d) and the complete desirability function D, which is the mathematical mean of the individual desirability esteems, is processed and improved. The desirability is characterized with the end goal that on the off chance that a reaction is past as far as possible, at that point the relating desirability worth will be 0. On the off chance that the reaction is on track, at that point the desirability worth will be equivalent to 1. At the point when the reaction falls inside the resistance span yet not on the objective, the comparing desirability will lie somewhere in the range of 0 and 1. As the reaction moves toward the objective, the desirability esteem turns out to be ever closer to 1. Individual desirability functions $d_i(\hat{y}_i)$ for each response $\hat{y}_i(k)$ is created by the fitted model and establishing the optimization criteria. Afterwards, depending on the optimization criteria, an acceptable range of response values is calculated by $U_i - L_i$, where U_i and L_i are the upper and lower values for the responses, respectively. In case of a minimization problem, $d_i(\hat{y}_i)$ is calculated by the following equation:

$$d_i(\hat{y}_i(\mathrm{x})) = \begin{bmatrix} 1 & if & \hat{y}_i(\mathrm{x}) < L_i \\ (\frac{U_i-\hat{y}_i(\mathrm{x})}{U_i-L_i})^n & if & L_i \le \hat{y}_i(\mathrm{x}) \le U_i \\ 0 & if & \hat{y}_i(\mathrm{x}) > U_i \end{bmatrix} \quad (10)$$

where n is the weight to determine how important is it for $\hat{y}_i$ to be close to the minimum.

4≤*Nap*≤8, 70≤V_c≤120 and mentioned cutting strategies conditions have been subjected to the problem to minimize the nose, right and left flank wear rate simultaneously. An equal importance of 3+ is devoted for all the objectives. The optimum cutting conditions are V_c=70 m/min, *Nap*=8, and left cutting strategy. The corresponding responses are W_{nose}=15.75 µm, W_{left}=10.25 µm and W_{right}=14 µm with a desirability of 0.997. Figure 5 demonstrates the desirability and optimization result graphs for the mentioned cutting strategy.

CONCLUSION

In this paper, the wear of the cutting tool during external threading operation of AISI 316L stainless steel using different cutting strategies and parameters has been studied. The below mentioned results have been obtained.

The highest flank wear on the top, on the right edge and on the left edge has been observed as 57 µm, 43 µm and 39 µm, respectively.
The lowest tool nose wear, flank wear on the right and left edge has been observed as 16 µm, 14 µm and 10 µm, respectively.

In general, minimum flank wear has been observed in the opposite way against to the feed direction. Although the flank wear on the right edge which is in the same direction with feed and is lower than the flank wear on the top of tool insert. Also, the cutting speed and depth of cut have significant effects on flank wear. According to the equations obtained in all conditions, it was observed that the flank wear increased as the cutting speed increased. At the same time, it has been observed that the tool wear increases as the depth of cut increases, but depth of cut has a positive effect for flank wear on the nose of the tool.
Empirical equations have been developed in order to predict the wear rate in the cutter for each strategy. The threading has been focused on through desirability optimization method. According to the optimization results, the lowest tool wear occurs in left mode, 70 m/min of cutting speed and 8 passes of cut.

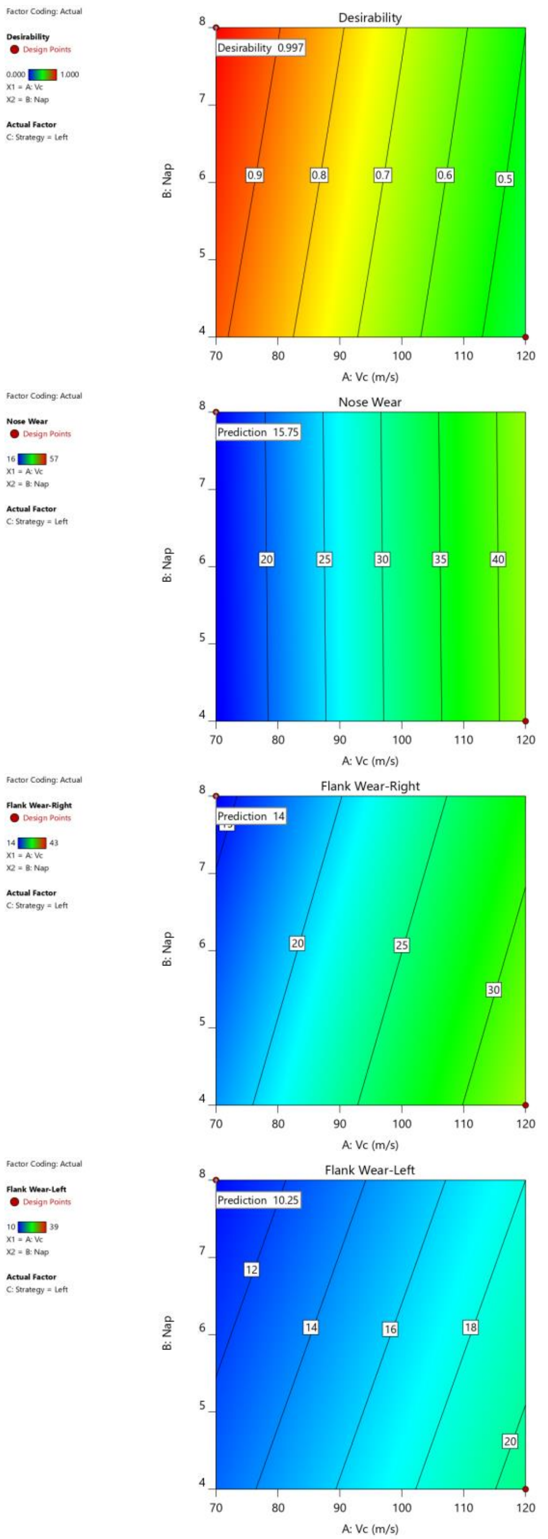

Figure 5. The desirability and optimization result graphs

ACKNOWLEDGEMENTS

The authors thank TUBITAK (The Scientific and Technological Research Council of Turkey) for partially supporting this work under project number 118C069.

ÖZET

Erkek diş çekme, talaşlı imalat süreçlerinde en önemli operasyonlardan birisidir. Mikro ölçekte takım geometrileri, yeni kaplama malzemeleri ve kaliteleri dahil olmak üzere yeni teknolojilerin ve bilgilerin geliştirilmesine rağmen, paslanmaz çelik gibi işlenmesi zor malzemelerin diş çekme operasyonlarında, takım aşınması hızla artmaktadır ve takım ömrü birkaç dakika kadar kısa olabilmektedir. Ayrıca, takım aşınması, iş parçasının geometrik doğruluğunu ve yüzey kalitesini etkilemektedir. Mevcut çalışma, AISI 316L paslanmaz çeliğin erkek diş çekme işlemi sırasında farklı kesme stratejileri ve parametrelerinin takım aşınması üzerindeki etkilerini araştırmaktadır. Aşınma oranı ve mekanizması, kesici takımın burnunda, kesme kenarlarının solunda ve sağında olarak değerlendirilmiştir. Takım aşınma sorunu, istenebilirlik fonksiyonu optimizasyon yöntemi ile değerlendirilmiştir.

Anahtar Kelimeler: Diş çekme, kesme stratejileri, takım aşınması, optimizasyon.

REFERENCES

1. M. Yasir, T. L. Ginta, B. Ariwahjoedi, A. U. Alkali, M. Danish, Effect of cutting speed and feed rate on surface roughness of AISI 316l ss using end-milling, ARPN Journal of Engineering and Applied Sciences, Vol. 11, No. 4, 2016
2. Ezugwu, E.O.; Okeke, C.I.; Machado A.R. (1998) High speed threading of inclusion-modified steels with coated carbide tools. Journal of Materials Processing Technology, 86: 216–222.
3. B. Siqueira, S.A. Freitas, R. B. D. Pereira, C. H. Lauro, L. C. Brandão, Influence of chip breaker and helix angle on cutting efforts in the internal threading process, The International Journal of Advanced Manufacturing Technology, 2019
4. R. C. E. Júnior, R. B. D. Pereira, C. H. Lauro, L. C. Brandão, Research on the wear mechanisms during the high-speed tapping in 316L stainless steel, The International Journal of Advanced Manufacturing Technology, 2020
5. Ondin O, Kıvak T, Sarıkaya M, Yıldırım V (2020) Investigation of the influence of MWCNTs mixed nanofluid on the machinability characteristics of PH 13-8 Mo stainless steel. Tribol Int 148:106323
6. I. C. Pereira, M. B. da Silva, Study of the internal thread process with cut and form taps according to secondary characteristics of the process, Int J Adv Manuf Technol, 2017

7. H. K. Akyildiz, H. Livatyali, Prediction and experimental analysis of cutting forces during machining of precision external threads, Machining Science and Technology, 2011, 15:485–506
8. Astakho, V.P. (2004) The assessment of plastic deformatio in metal cutting. Journal of Materials Processing Technology, 146: 193–202.7. H. Kato, S. Nakata, N. Ikenaga, H. Improvement of chip evacuation in drilling of lead-free brass using micro drill, International journal of automation technology, 8; 2014.
9. https://www.viraj.com/admin/sites/default/files/Viraj-Profiles-Catalogue_0.pdf
10. Espritcam 2017 commerical software help/DP Technology
11. http://www.helmancnc.com/fanuc-31i-g-codes-machining-center-fanuc-30i-31i-32i/
12. https://www.mmsonline.com/articles/threading-on-a-lathe
13. L. V. Candioti, M. M. De Zan, M. S. Cámara, H. C. Goicoechea, Experimental design and multiple response optimization. Using the desirability function in analytical methods development, Talanta Volume 124, 15 June 2014, 123-138